Evaluation of Small-Scale Laterally Loaded Monopiles in Sand

H. R. Roesen, K. Thomassen, S. P. H. Sørensen & L.B.Ibsen
Department of Civil Engineering – Aalborg University, Aalborg, Denmark

2011 Pan-Am CGS Geotechnical Conference

ABSTRACT
In current designs of offshore wind turbines, monopiles are often used as foundation. The behaviour of the monopiles when subjected to lateral loading has not been fully investigated. In this paper the diameter effect on laterally loaded non-slender piles in sand is evaluated by means of results from six small-scale laboratory tests, numerical modelling of the same test setup and existing theory. From the numerical models, *p–y* curves are derived and compared to current design regulations. The recommendations in API (1993) and DNV (1992) are observed to be in poor agreement with the numerically obtained *p–y* curves. The initial stiffness, E_{py}*, of the *p–y* curves is found to increase with increasing pile diameter. Considerable uncertainties are observed to be related to small-scale testing, and the evaluations clearly indicate that the accuracy of small-scale testing is increased when increasing the pile diameter and applying overburden pressure.

PRESENTACIONES TÉCNICAS
En el actual diseño de turbinas eólicas marinas, mono-pilas son generalmente usadas como cimentación. El comportamiento de las mono-pilas sometidas a cargas laterales no ha sido completamente investigado. En este articulo, la influencia del diámetro en pilas no esbeltas sujetas a cargas laterales es evaluada a través de 6 test de laboratorio a pequeña escala, modelos numéricos de los propios test y el uso de la teoría existente. Del los modelos numéricos, las curvas *p-y* son obtenidas y comparadas con la actual normativa de diseño. Las recomendaciones de la API (1993) y DNV (1992) muestran una pobre similitud con las curvas *p-y* obtenidas de forma numérica. Se ha hallado que la rigidez inicial, E_{py}* de las curvas *p-y* incrementa con el incremento de diámetro de la pila. Además, se hallan incertidumbres considerables relacionadas con los test a pequeña escala, y la evaluación de los mismos indica claramente que la precisión de los test a pequeña escala se ve incrementa cuando el diámetro de la pila y la presión de sobrecarga son incrementadas.

1 INTRODUCTION

In the design of laterally loaded monopiles, the *p–y* curve method, given by the design regulations API (1993) and DNV (1992), is often used. For piles in sand, the recommended *p–y* curves are based on results from two slender, flexible piles with a slenderness ratio of L/D = 34.4, where L is the embedded length and D is the diameter of the pile. (Reese et al., 1974) Contrary to the assumption of flexible piles for these curves, the monopile foundations installed today have a slenderness ratio L/D < 10 and behave almost as rigid objects. The recommended curves do not take the effect of the slenderness ratio into account. Furthermore, the initial stiffness is considered independent from the pile properties such as the pile diameter. The research within the field of diameter effects gives contradictory conclusions. Different studies have found the initial stiffness to be either independent, linearly dependent, or non-linear dependent on the pile diameter, cf. Ling (1988), Fan and Long (2005), and Lesny and Wiemann (2006).

The aim of this paper is to evaluate the diameter effect on the pile soil interaction. Six small-scale tests on laterally loaded monopiles in sand have been conducted; cf. Thomassen et al. (2011). The diameter effect is evaluated by comparing results from these tests with calibrated numerical models of the same test setup and with existing theory. Furthermore, *p–y* curves recommended in the current design regulations API (1993) and DNV (1992) are compared to curves obtained from the numerical models. As the foundations for offshore wind turbines are sensitive towards rotation and vibrations, strict demands for the stiffness of the foundation are induced. Therefore, the diameter effect is evaluated with focus on the initial stiffness of the *p–y* curves.

2 LABORATORY TEST SETUP

Six quasi-static tests on two closed-ended aluminium piles with a wall-thickness of 5 mm and outer diameters of 40 mm and 100 mm, respectively, have been conducted. The piles had a slenderness ratio, L/D, of 5 corresponding to embedded lengths of 200 mm and 500 mm. The piles were installed in 580 mm fully saturated sand. The aim of the tests was to obtain load-deflection relationships for the piles. Therefore, the piles were loaded laterally 370 mm above the soil surface, and the deflection of the pile was measured at three levels above soil surface, cf. Figure 1.

In order to minimize errors such as small non-measurable stresses and a non-linear failure criterion, the tests were conducted in a pressure tank. The effective stresses in the soil were increased by placing an elastic membrane on the soil surface sealing the soil from the upper part of the pressure tank. When increasing the pressure in the upper part of the tank, the membrane was pressed against the soil leading to an increase of the stresses in the soil. The lower part of the tank was

connected to an ascension pipe ensuring that the load was applied only as contact pressures between the grains. The tests were conducted at stress levels of 0 kPa, 50 kPa, and 100 kPa. The soil parameters were determined from cone penetration tests in accordance with Ibsen et al. (2009). A detailed description of the laboratory tests can be found in Thomassen et al. (2011).

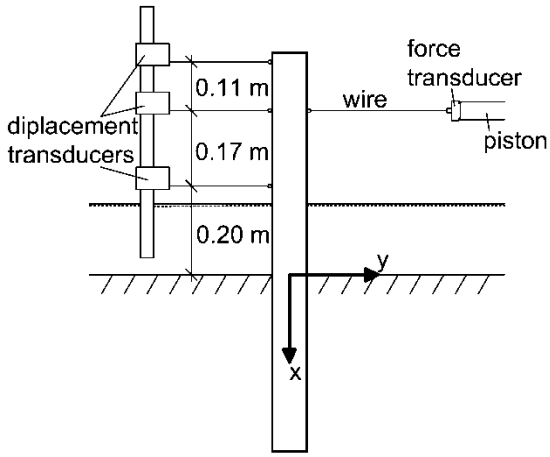

Figure 1. Setup for measuring the lateral deflection of the pile at three levels. The measurements are in mm.

3 NUMERICAL 3D MODELS

The six laboratory tests are modelled in the commercial, explicit finite difference program FLAC^{3D} (Itasca, 2006). The modelling programme is chosen to match the testing programme in Thomassen et al. (2011), cf. Table 1.

Table 1. Modelling programme for the numerical models.

		Diameter D (mm)	Slenderness ratio L/D (-)	Overburden pressure P_0 (kPa)
Model 1	(Test 1)	100	5	0
Model 2	(Test 2)	100	5	50
Model 3	(Test 3)	100	5	100
Model 4	(Test 4)	40	5	0
Model 5	(Test 5)	40	5	50
Model 6	(Test 6)	40	5	100

The model geometry is set to match the conditions in the pressure tank. Therefore, the outer boundaries are specified as the volume of the soil mass in the tank, i.e. a diameter of 2.1 m and a soil depth of 0.58 m. The pile and soil are generated by use of predefined zone elements. Because large variations in strain and stresses occur in the soil near the pile a finer zone mesh is generated in this area. The zone geometry for the 100 mm pile is shown in Figure 2. In order to model a correct pile soil interaction an interface is generated between the pile and the soil by use of standard FLAC^{3D} interface element.

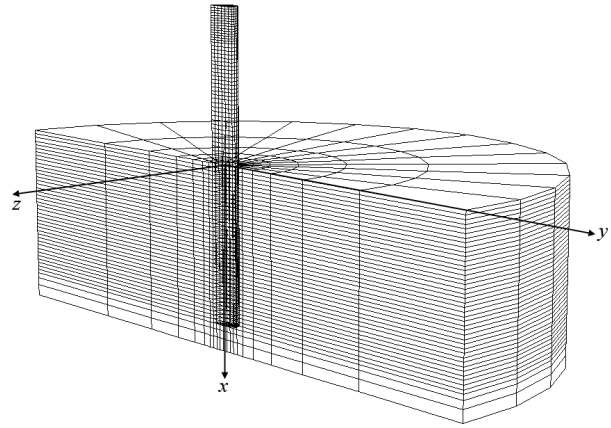

Figure 2. Zone geometry in the models with 100 mm pile.

At the outer perimeter of the soil the element nodes are restrained in the *y*- and *z*-direction, cf. Figure 2. At the bottom surface of the model the nodes are restrained in all directions. Due to axis-symmetry only half the laboratory setup is modelled and the nodes at the symmetry line are restrained in the *z*-direction.

The initial stresses are generated based on the density of the material, the gravitational loading, and the overburden pressure. The horizontal stresses are generated by use of a K_0-procedure in which $K_0 = 1 - \sin(\varphi_{tr})$

As a simplification, the piles are modelled as solid cylinders in contrast to the closed-ended pipe piles used in the laboratory tests. The solid piles are modelled with a reduced modulus of elasticity, E_{solid}, found by equating bending stiffness of the piles, cf. Equation 1.

$$E_{solid} = \frac{E_{hollow}\, I_{hollow}}{I_{solid}} \qquad [1]$$

I is the second moment of inertia, and the subscripts $_{hollow}$ and $_{solid}$ denote the parameters for the pipe piles in the laboratory tests and the parameters employed in the numerical models, respectively. In the same way, a reduced density is found by equating the cross-sectional areas and density of the hollow and solid pile.

3.1 Material Models and Properties

The constitutive relation in the soil is described by an elasto-plastic Mohr-Coulomb model in which tension cut-off is employed. The yield function is controlled by a non-associated flow rule. The piles are modelled by use of an elastic, isotropic model and the constitutive model for the interface is defined by a linear Coulomb shear-strength criterion.

The soil properties in the six models are defined equal to the findings of the six laboratory tests, cf. Table 2. Due

to the small variations in effective stresses through the soil layer the soil parameters are assumed to be constant with depth for all the models. Cohesion, *c*, of 0.1 kPa and Poisson's ratio, *v*, of 0.23 is applied for the soil in all six models.

For the tests without overburden pressure the low stresses lead to large uncertainties in the calculation of the initial tangential elasticity modulus, E_0. Thus, in the numerical models without overburden pressure E_0 is calibrated in relation to the initial stiffness of the load-deflection curves from the laboratory test. In the same way, the interface properties are calibrated. When using the interface properties listed in Table 3, the initial part of the load-deflection curves are found to be similar to the curves obtained in the laboratory tests.

Table 2. Soil properties determined by the six laboratory tests and employed in the numerical models. The elasticity moduli written in parentheses are found by means of the numerical model. (Thomassen et al., 2011)

	Friction angle φ_{tr} (°)	Dilation angle ψ_{tr} (°)	Effective unit weight of soil γ' (kN/m^3)	Modulus of elasticity E_0 (MPa)
Model 1	53.7	19.6	10.3	(4.0)
Model 2	50.3	19.0	10.4	38.2
Model 3	47.7	18.3	10.4	55.6
Model 4	54.4	20.4	10.4	(2.0)
Model 5	50.4	19.1	10.4	38.6
Model 6	48.0	18.6	10.4	57.2

Table 3**:** Interface properties calibrated by means of the numerical models.

Friction angle φ_{int} (°)	Dilation angle ψ_{int} (°)	Cohesion c_{int} (kPa)	Normal stiffness k_n (MPa)	Shear stiffness k_s (MPa)
30.0	0.1	0.0	100 x E_0	100 x E_0

3.2 Calculation Phase

During the calculation phase in the modelling the total lateral force, *H*, the displacement, *y*, and the stresses, *p*, along the pile are recorded. The bending moment, *M*, and soil pressure, *p*, are calculated based on the recorded stresses in the pile and the interface. The bending moment of the pile at a given level is calculated by use of Navier's formula. In order to eliminate the average vertical stress, corresponding to the axial force acting on the pile, the bending moment in each level is calculated by two points $(y,z) = (\pm D/2, 0)$. The soil resistance per unit length along the pile, p_y, is computed by integrating the stresses in the interface nodes along the interface circumference.

3.3 Calibration of the Numerical Models

The calibration of the numerical models is based on a comparison between the load-deflection curves obtained from the numerical models and the load-deflection curves obtained from the small-scale tests in the laboratory. In Figures 3 to 6 the curves for the 100 mm and 40 mm pile with P_0 = 0kPa and P_0 = 100 kPa, respectively, are shown.

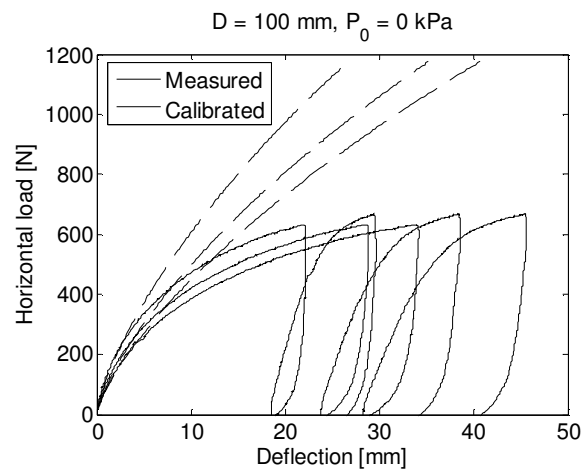

Figure 3. Calibrated and measured relationships at three levels above the soil surface for the test 100 mm with P_0 = 0 kPa.

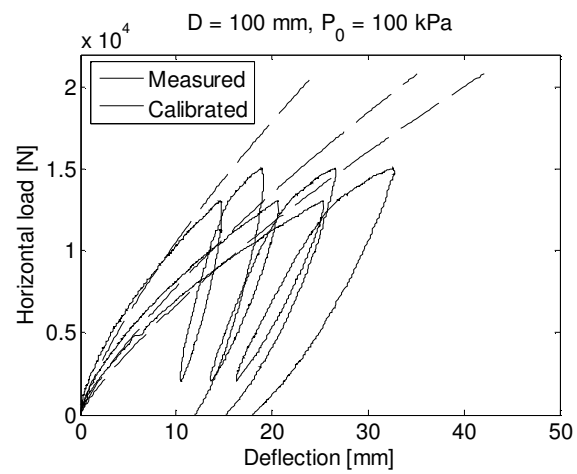

Figure 4. Calibrated and measured relationships at three levels above the soil surface for the test 100 mm with P_0 = 100 kPa.

In Figure 3 it he initial stiffness for the calibrated and the test curves are observed to be in agreement. However, the capacity of the calibrated model exceeds the capacity of the laboratory test. This indicates that the internal angle of friction, φ_{tr}, inserted in the model is overestimated. The same results are found when evaluating the 40 mm pile with P_0 = 0 kPa, cf. Figure 5. The reason for the disagreement in capacity is that φ_{tr} is

based on the CPTs conducted prior to each laboratory test. At low stress levels, φ_{tr} varies significantly with the stresses and it is difficult to determine φ_{tr} with sufficient accuracy. A calibration of φ_{tr} and ψ_{tr} has not been conducted but it would result in better agreement.

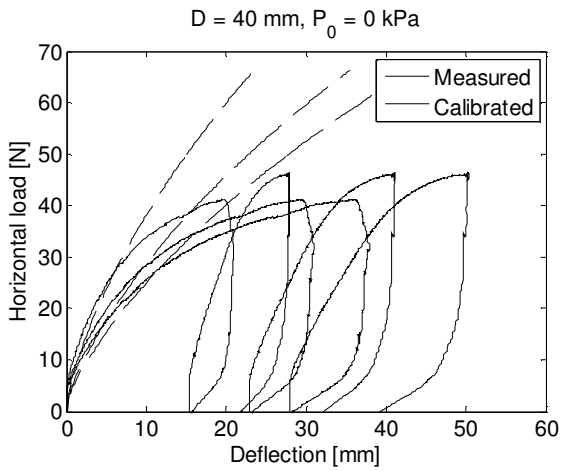

Figure 5. Calibrated and measured relationships at three levels above the soil surface for the test 40 mm with P_0 = 0 kPa.

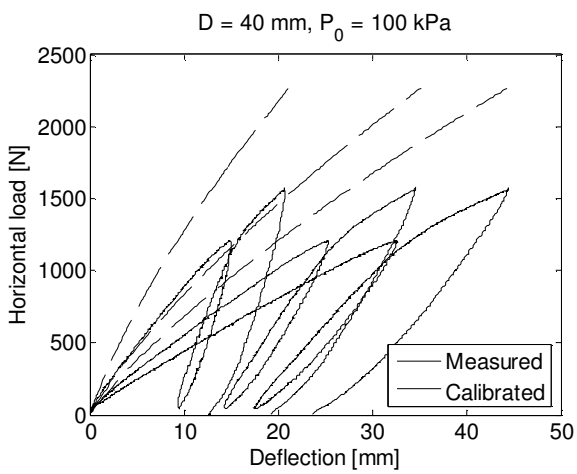

Figure 6. Calibrated and measured relationships at three levels above the soil surface for the test 40 mm with P_0 = 100 kPa.

In the models with overburden pressure applied the agreement between the capacity in the calibrated and the measured load-deflection relationship is found to increase with increasing pile diameter and increasing overburden pressure. Thus, the best agreement is found for the 100 mm pile with P_0 =100 kPa, cf. Figure 4.

Considerable uncertainties are related to the test results for the 40 mm pile, cf. Thomassen et al. (2011). Especially the model for P_0 = 100 kPa showed significant disagreement between the calibrated and the measured values, cf. Figure 6. This disagreement is explained by a disturbance of the soil prior to the test as described in Thomassen et al. (2011). The calibration of the six models indicates that the accuracy in small-scale testing is increased when applying overburden pressure.

4 EVALUATION OF RESULTS FROM NUMERICAL MODELS

The numerical results are evaluated to verify the expected deviations between the recommendations in the design regulations API (1993) and DNV (1992) and the results for non-slender piles with varying diameters.

4.1 Evaluation of Lateral Deflection

In Figure 7, the lateral deflection with depth at three different overburden pressures for the 100 mm pile is shown. The prescribed deflection at x = –370 mm is 35 mm and below the soil surface the deflection is recorded in 26 levels for the 100 mm pile. Above the soil surface, the deflection is recorded in two levels: x = –200 mm and x = –370 mm.

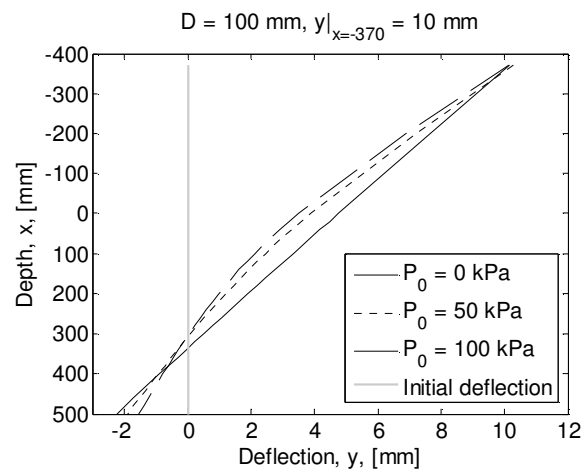

Figure 7. Lateral deflection with depth for different overburden pressures for the 100 mm piles.

When applying overburden pressure the pile exhibits a more flexible behaviour than without overburden pressure, cf. Figures 7. This is in accordance with Poulos and Hull (1989), who proposed a criterion for the pile-soil interaction in which an increase in the soil stiffness compared to the pile stiffness leads to a more flexible behaviour of the pile.

Although the piles behave more flexible when overburden pressure is applied, the primary deflection is caused by rigid body rotation, which is evident because only a single point of rotation and a negative deflection at pile toe is present. The same results are found for the 40 mm pile. This rigid behaviour is expected for the non-slender piles but it is in contrast to the flexible behaviour of piles which the design regulations are based on.

4.2 Evaluation of Diameter Effect on the *p-y* Curves

The *p–y* curves derived from the models with P_0 = 0 kPa, P_0 = 50 kPa, and P_0 = 100 kPa at three different depths 20 mm, 40 mm and 60 mm are shown in Figures 8 to 10.

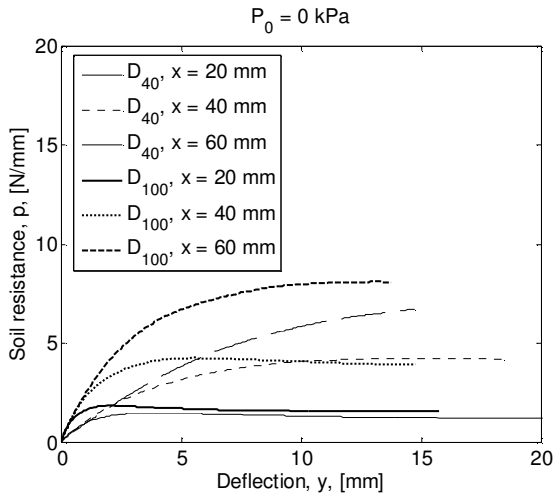

Figure 8. *p–y* curves at three different depths for models with 40 mm and 100 mm piles and P_0 = 0 kPa.

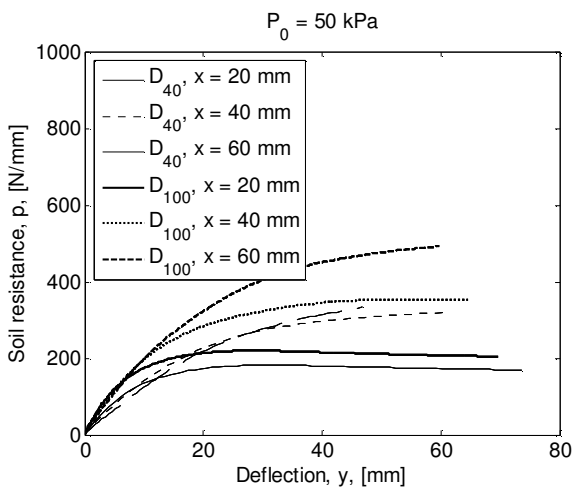

Figure 9. *p–y* curves at three different depths for models with 40 mm and 100 mm piles and P_0 = 50 kPa.

In Figure 8 at the depth of 20 mm, the ultimate soil resistance for the 100 mm pile is higher than for the 40 mm pile. At the depth of 40 mm, the opposite is the case. For the depth of 60 mm, the curve for the 40 mm pile seems to approach the ultimate soil resistance for the 100 mm pile. For the test with overburden pressure applied it is only possible to evaluate the ultimate resistance at the depth 20 mm due to the limited applied displacement, cf. Figures 9 and 10. Because of this limited displacement it is difficult to draw any clear conclusion regarding the diameter effect on the ultimate resistance.

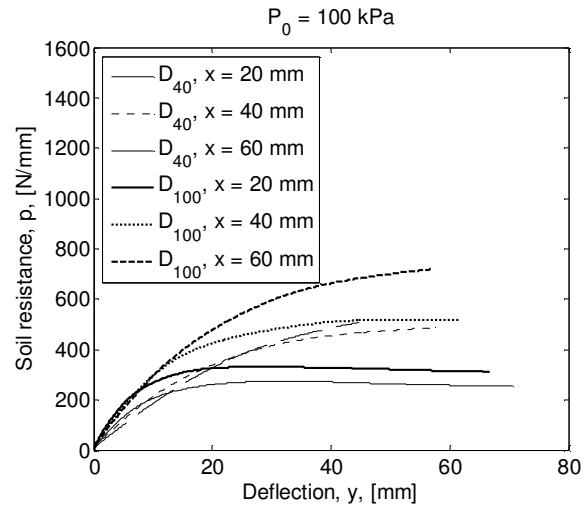

Figure 10. *p–y* curves at three different depths for models with 40 mm and 100 mm piles and P_0 = 100 kPa.

The initial stiffness of the curves is found to be dependent on the pile diameter, i.e. the larger pile diameter the higher initial stiffness, cf. Figures 8 to 10. This is in contrast to API (1993) and DNV (1992) in which the initial stiffness is considered independent on the pile diameter. The dependency of the diameter on the initial stiffness is evaluated further in Section 6.

5 COMPARISON OF DESIGN REGULATIONS AND NUMERICAL MODELS

To establish whether the recommendations in the design regulations API (1993) and DNV (1992) gives good estimations of the pile-soil interaction for non-slender piles, the design method and model results are compared.

It is not possible to take the overburden pressure into account in the formulations given by the design regulations. Thus, in the evaluation in Section 5.1 only the results from the tests without overburden pressures are included.

5.1 Evaluation of *p-y* Curves

The *p–y* curves recommended in the design regulations API (1993) and DNV (1992) are compared to the *p–y* curves obtained by the numerical models. For the two tests without overburden pressure the comparison is shown in Figures 11 and 12 for three different depths.

The figures show that the ultimate soil resistance recommended by API (1993) is significantly lower than the resistance obtained by the numerical models, most significant for the 40 mm pile, cf. Figure 12. This large difference is believed to occur because the capacity in the numerical models is overestimated compared to the test results. Hence, the difference emerges from uncertainties when determining the soil parameters for low stress levels.

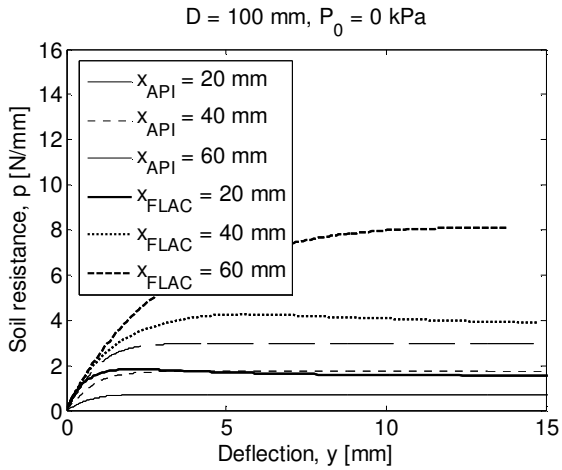

Figure 11. *p–y* curves for three depths from the numerical model and the design regulation formulation for the 100 mm pile with P_0 = 0 kPa.

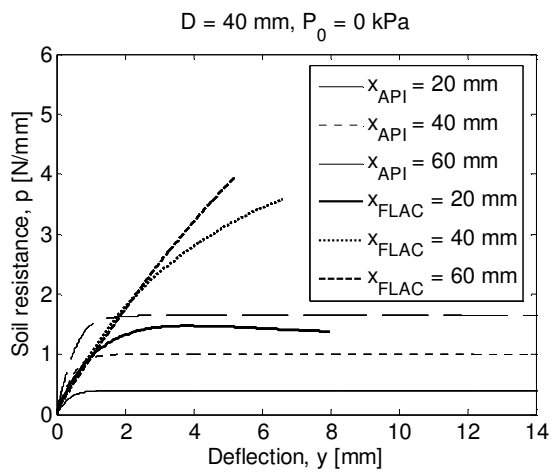

Figure 12. *p–y* curves for three depths from the numerical model and the design regulation formulation for the 40 mm pile with P_0 = 0 kPa.

In Figure 12, the initial stiffness of the *p–y* curves from the numerical models is seen to be in agreement with the calculated initial stiffness from the curve at a depth of 40 mm. In Figure 11, however, the initial stiffness of the *p–y* curves from the numerical models is in agreement with the calculated initial stiffness from the curve at 60 mm. Because the initial stiffness found by the numerical models is constant with depth in the evaluated depth interval and because of the difference between the initial stiffness in Figures 11 and 12, it is difficult to draw any clear conclusions in relation to the recommendations other than the agreement between the curves are poor.

6 EVALUATION OF INITIAL STIFFNESS

In API (1993) and DNV (1992) the initial stiffness of the *p–y* curves, E_{py}^*, given by Equation 2, is assumed to vary linearly with depth.

$$E_{py}^* = \frac{dp}{dy}\Big|_{y=0} = kx \qquad [2]$$

k is the initial modulus of subgrade reaction and *x* is the depth below soil surface. *k* is according to the design regulations dependent only on the relative density or the friction angle of the soil and, thus, independent of the pile properties. Because of strict demands for the maximum rotation of the wind turbines and the resonance in serviceability mode, the initial stiffness of the *p–y* curves are of great importance. Therefore, it is of interest to find a correct expression for the initial stiffness in order to find the correct pile deflection. Sørensen et al. (2009) proposed a non-linear formulation for the initial stiffness, cf. Equation 3, based on numerical simulations of full-scale monopiles in sand.

$$E_{py}^* = a\left(\frac{x}{x_{ref}}\right)^b \left(\frac{D}{D_{ref}}\right)^c \varphi_{tr}^d \qquad [3]$$

a = 50000 kN/m^2 for (x,D,φ_{tr}) = (1 m, 1 m, 1 rad) and the constants (b,c,d) = (0.6, 0.5, 3.6). x_{ref} and D_{ref} are reference values both of 1 m. Similar to API (1993), the initial stiffness increases with increasing internal angle of friction, however with a slightly different variation. Contrary to API (1993), the initial stiffness increases with increasing pile diameter and varies non-linearly with depth when using Equation 3.

6.1 Comparison of Load-Deflection Relationships from Design Regulations, Non-linear Theory and Tests

To compare the test results to the recommendations given by the design regulations, API (1993) and DNV (1992), a traditional Winkler model is made in MATLAB by using the finite element toolbox CALFEM.

For the non-linear theory Equation 3 is inserted in the formulation for the soil resistance given in API (1993) and employed in the Winkler model. Thereby, the load-deflection relationships shown in Figures 13 and 14 for the two piles without overburden pressure are obtained.

For the 40 mm pile, cf. Figure 14, it is difficult to determine which of the formulations is the best fit for the test results as these results are positioned in between the two. Moreover, because of the large uncertainties for this test, the results may not be representative for the correct pile-soil behaviour.

The uncertainties for the test results with the 100 mm pile are smaller, and the results are considered more accurate. Figure 13 shows that the formulation by API (1993) overestimates the lateral capacity. When using the non-linear formulation for the initial stiffness, the lateral capacity is closer to the measured results, however still overestimated. For the initial part of the curves, the non-linear expression is seen to be in better agreement with the results obtained in the laboratory tests and, therefore, the non-linear expression is believed to give the best estimate of the variation of the initial stiffness.

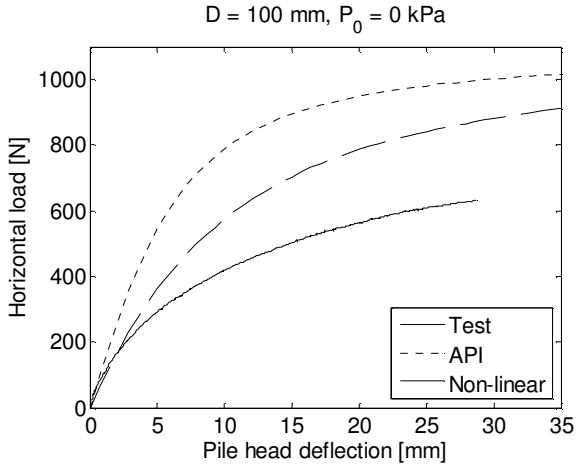

Figure 13. Load-deflection relationships measured at the height of the hydraulic piston (x = –370 mm) obtained from the tests and the Winkler model approach with the expressions for the ultimate soil resistance with both linear and non-linear formulation of the initial stiffness incorporated. D = 100 mm. P_0 = 0 kPa. The initial modulus of subgrade reaction, k, is set to 40000 kN/m^3.

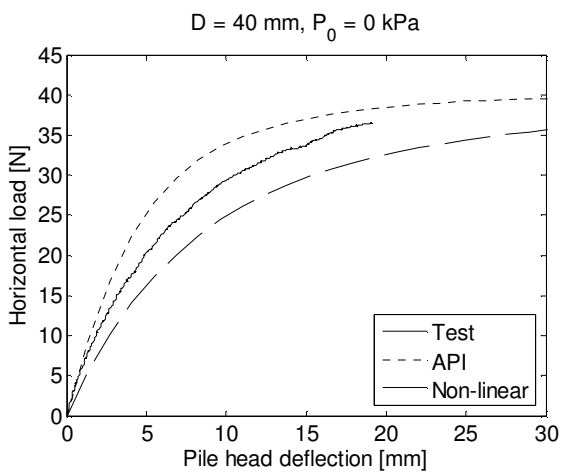

Figure 14. Load-deflection relationships measured at the height of the hydraulic piston (x = –370 mm) obtained from the tests and the Winkler model approach with the expressions for the ultimate soil resistance with both linear and non-linear formulation of the initial stiffness incorporated. D = 40 mm. P_0 = 0 kPa. The initial modulus of subgrade reaction, k, is set to 40000 kN/m^3.

6.2 Comparison of Initial Stiffness from Numerical Models and Non-linear Theory

In order to evaluate the diameter effect the non-linear formulation for the initial stiffness, Equation 3, is evaluated in comparison to the initial stiffness found from the p–y curves from the six numerical models. The factor c is evaluated by the ratios:

$$\frac{E_{py}^{*}\,|_{D=100}}{E_{py}^{*}\,|_{D=40}} = \left(\frac{D_{100}}{D_{40}}\right)^{c} \qquad [4]$$

The initial stiffness of the numerically obtained p–y curves, cf. Figures 8 to 10, is found by linear regression of the data until a deflection of approximately 0.2 mm. The slope of the linear regression is assumed representative for the initial stiffness, and the obtained values for the six models are shown in Table 4.

Table 4. The initial stiffness read of the p–y curves obtained from the numerical models for the two piles at different overburden pressures, cf. Figures 8 to 10.

Overburden Pressure:	0 kPa	50 kPa	100 kPa
$E_{py}^{*}/_{D=100}$ (N/mm^2)	2.9	42.3	79.2
$E_{py}^{*}/_{D=40}$ (N/mm^2)	1.3	30.0	48.9

With c = 0.5, as proposed by Sørensen et al. (2010), the right side of Equation 4 gives approximately 1.6. If this value of c is correct, the ratio on the left side of the equation should give values of approximately 1.6 as well. In Table 5, the ratios of the initial stiffness from the numerical models are given. The ratio for the models without overburden pressure deviates the most. The ratios for the models with overburden pressure indicate that c = 0.5 is an appropriate value for the diameter effect on the initial stiffness. The results in Table 5 indicate that larger uncertainties are related to the tests without overburden pressure and, hence, low stress levels in the soil.

Table 5. Ratio of the initial stiffness of the p–y curves obtained in the numerical models for the different overburden pressures.

Overburden Pressure:	0 kPa	50 kPa	100 kPa
$\frac{E_{py}^{*}\,\|_{D=100}}{E_{py}^{*}\,\|_{D=40}}$	2.3	1.4	1.6

7 CONCLUSION

In this paper, the diameter effect on the pile-soil interaction is evaluated by means of results from small-scale laboratory tests, numerical models of the same test setup, and existing theory. In total, six tests were carried out on piles with outer diameters of 40 mm and 100 mm, respectively, and a slenderness ratio L/D of 5. In four of the tests, overburden pressures of 50 kPa and 100 kPa were applied. The tests were modelled in the numerical finite difference program FLAC^{3D}, and the models were calibrated against the obtained load-deflection relationships from the laboratory tests. From the numerical models, p–y curves for the six tests were obtained and used in a comparison to the recommended

curves in the current design regulations. From the evaluations, the following conclusions can be drawn:

In the numerical models the recorded deflection along the pile when subjected to lateral loading showed an increase in flexible behaviour when overburden pressure was applied. However, the primary deflection of the piles was caused by rigid body rotation.

Based on a comparison of the *p–y* curves for the two pile diameters, the initial stiffness, $E_{py}*$, is found to increase with increasing pile diameter. The dependency of the diameter was further evaluated by means of $E_{py}*$ obtained in the numerical models and by the non-linear formulation suggested in Sørensen et al. (2010). The models with overburden pressure indicated that a value of c = 0.5 for the diameter dependency is an appropriate value. By employing the formulation in a Winkler model approach the non-linear formulation was compared to the tests results and it was found that this formulation was in better agreement with the test results than the formulations given in API (1993) and DNV (1992) where $E_{py}*$ is assumed independent of pile diameter.

In the calibration of the numerical models, the evaluation of *p–y* curves, and the evaluation of $E_{py}*$ considerable uncertainties are found to be related to small-scale testing. The evaluations clearly indicate that the accuracy in small-scale testing increases when increasing pile diameter and applying overburden pressure.

ACKNOWLEDGEMENTS

The project is associated with the EFP programme “Physical and numerical modelling of monopile for offshore wind turbines”, journal no. 033001/33033-0039 and the EUDP programme “Monopile cost reduction and demonstration by joint applied research”. The funding is sincerely acknowledged.

REFERENCES

API 1993. *Recommended Practice for Planning, Designing and Constructing Fixed Offshore Platforms - Working Stress Design*, American Petroleum Institute.

DNV 1992. *Det Norske Veritas -Foundations*, Det norske veritas Classification A/S, Høvik, Norway.

Fan C. C., and Long J. H., 2005. Assessment of existing methods for predicting soil response of laterally loaded piles in sand. *Computers and Geotechnics* 32: 274-289.

Hansen, J. B. 1961. *The Ultimate Resistance of Rigid Piles Against Transversal Forces*, Bulletin No. 12. The Danish Geotechnical Institute, Copenhagen, Denmark.

Ibsen, L. B., Hanson, M., Hjort, T. And Thaarup, M. 2009. MC-Parameter Calibration for Baskarp Sand No. 15, *DCE Technical Report No. 62*, Aalborg University, Denmark.

Itasca Consulting Group Inc. 2006 *Fast Langrangian Analysis of Continua in 3 Dimensions*, Minneapolis, Minnesota, USA.

Lesny, K. and Wiemann, J. 2006. Finite-Element-Modelling of Large Diameter Monopiles for Offshore Wind Energy Converters, *Geo Congress 2006*, Atlanta, GA, USA

Ling L. F., 1988. *Back Analysis of Lateral Load Test on piles. Rep. No. 460*, Civil Engineering Dept., University Of Auckland, New Zealand.

Poulos, H. and Hull, T. 1989. The Role of Analytical Geomechanics in Foundation Engineering, *Foundation Engineering: Current principles and practice, 2*: 1578-1606.

Reese, L. C., Cox, W. R. and Koop, F. D. 1974. Analysis of Laterally Loaded Piles in Sand, *Offshore Technology Conference*. Houston, Texas, USA.

Sørensen, S., Ibsen, L. and Augustesen, A. 2010. *Effects of diameter on initial stiffness of p-y curves for large-diameter piles in sand*. unpublished, Aalborg University, Denmark.

Sørensen, S., Møller, M., Brødbæk, K., Augustesen, A. and Ibsen, L. 2009. Numerical Evaluation of Load-Displacement Relationships for Non-Slender Monopiles in Sand, *DCE Technical Report No. 80*. Aalborg University, Denmark.

Thomassen, K., Roesen, H. R., Ibsen, L. and Sørensen, S. 2011. Small-Scale Testing of Laterally Loaded, Non-Slender Monopiles in Sand, Submitted for publication in *2011 Pan-Am CGS Geotechnical Conference*, Aalborg University, Denmark.